Surface Modification of Thermoplastic Electrodes for Biosensing Applications via Copper-Catalyzed Click Chemistry

Brandaise Martinez, Yann R. Leroux, Philippe Hapiot, Charles S. Henry

Surface Modification of Thermoplastic Electrodes for Biosensing Applications via Copper-Catalyzed Click Chemistry

Brandaise Martinez[a], *Yann Leroux*[b], *Philippe Hapiot*[b], *Charles S. Henry*[a*]

[a] Department of Chemistry, Colorado State University, Fort Collins, Colorado, 80523-1872, USA

[b] Univ Rennes, CNRS, ISCR – UMR 6226, F-35000 Rennes, France

ABSTRACT: Cu(I)-catalyzed 1,3-dipolar cycloaddition (CuAAC), aka click chemistry, has been demonstrated to be highly robust while providing versatile surface chemistry. One specific application is biosensor fabrication. Recently, we developed thermoplastic electrodes (TPEs) as an alternative to traditional carbon composite electrodes in terms of cost, performance, and robustness. However, their applications in biosensing are currently limited due to lack of facile methods for electrode modification. Here, we demonstrate the feasibility of using CuAAC following diazonium grafting of thermoplastic electrodes (TPEs) to take advantage of two powerful technologies for developing a customizable and versatile biosensing platform. After performing a stepwise characterization of the electrode modification procedures, electrodes were modified with model affinity reagents. Streptavidin and streptavidin-conjugated IgG antibodies

were successfully immobilized on the TPE surface as confirmed by electrochemical impedance spectroscopy (EIS) and X-ray photoelectron spectroscopy (XPS).

KEYWORDS: Biosensor, electrode modification, carbon composite electrodes, electrochemical sensor, click chemistry

INTRODUCTION

Thermoplastic electrodes (TPEs) have been shown to have a wide range of applications including ion-selective electrodes, *Escherichia coli* sensors, and enzymatic glucose sensors.[1-6] The advantage of using these carbon composite electrodes is they are robust and yield better electrochemistry than other carbon electrodes, such as screen printed carbon electrodes (SPCEs), while being less expensive than traditional precious metal electrodes.[1] However, there is a gap in the ability to modify TPEs consistently and reliably for biosensing applications, particularly for immobilization of biorecognition elements such as antibodies and aptamers. Passive adsorption methods for antibody immobilization tend to be inconsistent due to the relatively weak intermolecular forces between the antibody and the electrode surface.[7] Covalent modification lends stronger binding and can help orientate antibodies to be able to bind the antigen. One commonly used covalent approach is (EDC)/N-hydroxysuccinimide (NHS) crosslinking.[5, 7-9] EDC/NHS has been shown to be successful on TPEs for *E. coli* detection, however, EDC/NHS chemistry can be prone to undesirable side reactions with water, primary amines, and carboxyl groups present in the system.[5, 10, 11] Thus, there is still a need for facile antibody immobilization, applicable to the highly variable surface topography and chemistries of TPEs.

Click chemistry, Cu(I)-catalyzed 1,3-dipolar cycloaddition (CuAAC), is an attractive solution and has been used in a wide variety of applications on precious metal and carbon electrodes.[12, 13]

The key to click chemistry is adding alkyne or azide functional groups on the electrode surface, which can be achieved via electroreduction of aryl diazonium ions.[14-17] Several groups have successfully applied CuAAC combined with diazonium grafting for biosensing applications on carbon electrodes using aptamers or antibodies as the biorecognition elements.[18-23] For instance, Sánchez-Tirado, *et. al.,* used alkyne-terminated IgGs to detect transforming growth factor β1 (TGF-β1) cytokine using multi-walled carbon nanotube modified SPCEs to achieve pg/mL limits of detection.[24] Success using SPCEs bolsters the motivation for exploring the CuAAC modification approach on TPEs.

One of the greatest advantages of the CuAAC approach to electrode surface modification is that it is easily customizable in terms of functional groups, pattern, film thickness, and can be performed under mild conditions.[25-27] The present study seeks to examine the performance of TPEs as an alternative to traditional electrodes with CuAAC modification following diazonium grafting as a platform for biosensing applications. Initial work using aryl diazonium grafting on TPEs was successful using organic solvents.[28] However, better electrochemical performances and easier fabrication are seen using TPE materials (polystyrene binder and polymethylmethacrylate template) that are not compatible with these solvents.[1] Diazonium grafting in water is established to be successful on TPEs here along with subsequent click chemistry based modification with a biotin moiety for easy linkage to streptavidin conjugated nanoparticles and antibodies as a proof of concept. The multistep process allows for a well-organized monolayer film to form as a result of the aryl diazonium grafting to form a convenient linkage point for the secondary click chemistry reaction.[15]

MATERIALS & METHODS

Electrochemical Characterizations

Thermoplastic electrodes (TPEs) made of TC303 carbon (Asbury Graphite Mills Inc, NJ) and 45,000 MW polystyrene (Sigma-Aldrich, St. Louis, MO) in polymethylmethacrylate (PMMA) templates were fabricated as previously reported.[1, 4] They were prepared for each experiment by wet sanding for 30 s each in a figure-eight pattern on silicon carbide sandpaper at 150 then 600 grit. They were then sonicated in ultrapure water for 5 min and air dried before use. All electrochemical measurements were performed with Palmsens4 potentiostat (Palmsens, Houten, Netherlands). Each electrode in the 3-electrode system (counter, working, and pseudo reference) were made of the same thermoplastic electrode material with 3 mm diameter working and reference electrodes and 4.5 mm counter electrode. All data was processed and plotted using MATLAB, unless otherwise specified.

Cyclic voltammograms (CVs) were collected by adding 300 μL of 1 mM $Fe(CN)_6^{3-/4-}$ (0.5 mM of potassium hexacyanoferrate trihydrate and 0.5 mM of potassium ferricyanide, Sigma Aldrich, St. Louis, MO) in 0.1 M KCl (99.0% Sigma Aldrich, St. Louis, MO) to the electrode system and scanning at 5, 10, 20, 40, 60, 80, 100, 300, and 500 mV/s in random order. Each scan rate was tested in triplicate on separate electrodes and the process was repeated in triplicate for 1 mM ferrocenedimethanol ($Fc(MeOH)_2$, Ambeed, Arlington Heights, IL) in 0.1 M KCl.

Electrochemical impedance spectroscopy (EIS) was performed in 10 mM $Fe(CN)_6^{3-/4-}$ in 0.1 M KCl with a fixed scan type at AC potential of 0.2 V with an equilibration time of 3 s. Frequency was scanned from 0.1 Hz to 10^5 Hz with 10 points taken per frequency decade. Fits were made to the equivalent circuit using PSTrace v.5.

Surface Characterizations

Scanning electron microscopy (SEM) was used to image surfaces. Representative TPE surfaces were sputter-coated to a 10 nm thick gold layer. Secondary electron images (SEI) were collected on a JEOL JSM-6500 Field Emission Scanning Electron Microscope with 10.0 kV accelerating voltage applied. All resulting images were processed in ImageJ software. For optical profilometry measurements, a Zygo ZeScope profilometer was used with 20x magnification and ZeMaps data acquisition software. X-ray photoelectron spectroscopy (XPS) was performed on a Physical Electronics X-Ray Photoelectron Spectrometer equipped with monochromated Al anode producing Al k_α x-rays and 0.8 x 0.8 mm aperture, 20 μA electron neutralizer, and argon ion gun neutralizer. Resulting high resolution spectra were processed and analyzed via CasaXPS software.

Scanning electrochemical microscopy (SECM) was performed using a CH Instruments 920D model and 10 um diameter Pt probe, with Ag/AgCl reference, and platinum wire counter electrode in a traditional three component system. The TPE surface was unbiased and tilt corrections were done using probe approach curves on the insulating electrode template surrounding the TPEs. Either 1 mM potassium ferrocyanide or 1 mM ferrocene dimethanol in 0.5 M KCl were used as the probe. Maps were processed using CH Instruments software and probe approach curves were fit using simulations via MIRA software.

Electrode modification

Electrode modification throughout this work follows the general steps shown in **Scheme 1**. First, the 4-(trimethylsilyl)ethynylbenzene diazonium salt was generated *in situ* from addition of 2 molar equivalents of sodium nitrite (99.99% metals basis, Sigma-Aldrich, St. Louis, MO) to 10

mM of 4-(trimethylsilyl)ethynylaniline (96%, Sigma-Aldrich, St. Louis, MO) in 0.1 M HCl (ACS certified, Fisher Scientific, Waltham, MA).[29] The diazonium solution was then diluted 20-fold in 0.1 M HCl. A 100 µL aliquot was added to the TPE and electroreduction of aryl diazonium ions was performed by CV by sweeping the potential from 0 to -0.8 V with a scan rate of 50 mV/s for five cycles[15] (**Scheme 1, Step 1**). Electrodes were rinsed thoroughly with MQ water and air dried before deprotection. Grafted electrodes were used within three days of electrografting (stored on benchtop protected from dust). The trimethylsilyl (TMS) protecting group was removed (**Scheme 1, Step 2**) via 20 min of sonication in 1 M of NaOH (Fisher Scientific, Waltham, MA). Electrodes were rinsed thoroughly with MQ water and air dried prior to the "click" reaction.

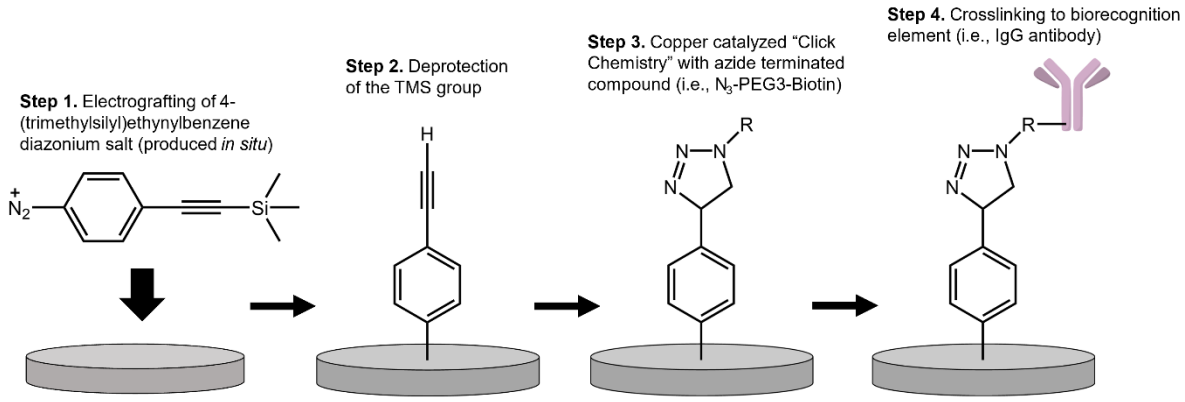

Scheme 1. Modification workflow for the covalent functionalization of thermoplastic electrodes.

Alkyne-azide cycloaddition click chemistry was performed next (**Scheme 1, Step 3**) with 20 mM of $CuSO_4$ (pentahydrate, 99%, Sigma-Aldrich, St. Louis, MO), 2.5 µL/mL of N_3-PEG3-N_3 (Toronto Research Chemicals, Toronto, ON) or 20 mM of N_3-PEG3-biotin (98%, BroadPharm, San Diego, CA), and 5 mM of L-ascorbic acid (Biogems International, Westlake Village, CA). A 25 µL of each reagent was added sequentially to the working electrode only and allowed to sit at

room temperature for 1 hour before rinsing with MQ water and air drying. A second click reaction was completed for electrodes modified with N_3-PEG3-N_3 with the same $CuSO_4$ and L-ascorbic acid (AA) with 20 mM of ethynylferrocene (Ambeed, Arlington Heights, IL). Concentrations of $CuSO_4$, AA, and N_3-PEG3-N_3 were optimized by determining peak signal and surface coverage, Γ_{Fc}, after clicking ethynylferrocene to the surface (**Figure S1**). Optimizations followed expected trends, where higher concentrations yielded higher surface coverage, except in the case of AA where the low pH of the higher concentration is hypothesized to have impeded the reaction.[30]

After click reactions (**Scheme 1, Step 4**), electrodes were successively rinsed with saturated EDTA solution (pH = 8) and water (optimization available in **Figure S2**). Electrodes modified with N_3-PEG3-biotin were incubated with 25 µL of 10 µg/mL of streptavidin (AnaSpec Inc., Fremont, CA, USA) or streptavidin-conjugated anti-*E. coli* IgG (Abcam, Cambridge, UK) for 30 minutes at room temperature. Anti-*E. coli* antibodies were linked to streptavidin prior to use via Lightning Link Kit (Abcam, Cambridge, UK). After incubation, the electrodes were rinsed thoroughly with water. All electrodes were used the same day that they were modified.

RESULTS & DISCUSSION

The surfaces of unmodified thermoplastic electrodes (TPEs) were first characterized to evaluate the composition and morphology prior to functionalization. **Figure 1A** shows SEM micrographs of the TPEs used in this study. The rough surface observed here is due to the polishing process applied to the TPEs before use. Through **Figure 1B**, the electrodes were determined to have a root-mean-square roughness of the representative surface sample of R_{RMS} = 0.776 µm (average roughness, R_A = 0.575 µm). This is more than previously reported roughness values for commercial screen-printed carbon electrodes (R_A = 0.121 µm).[31] It was hypothesized

that these TPEs yield high electrochemical performance due to the abundance of edge planes at the surface,[32] which effectively enhances the surface area available to electrochemical reactions. **Figure 1C** shows the C1s high resolution x-ray photoelectron spectrum of the TPE surface. The thermoplastic binder, polystyrene, is the primary contributor to the C1s spectrum.[33] The C1s spectrum can be peak-fitted in 3 main contributions at 284.9 eV, 285.4 eV, and 286.8 eV corresponding to C-C, C=C (50.5%), C-O (26.5%) and C=O (23.0%). The oxygen to carbon ratio (I_O/I_C) based on the XPS survey spectrum (**Figure S4**) is 0.067 which is expected based on the individual spectra of the electrode components: graphite and polystyrene.[34-36]

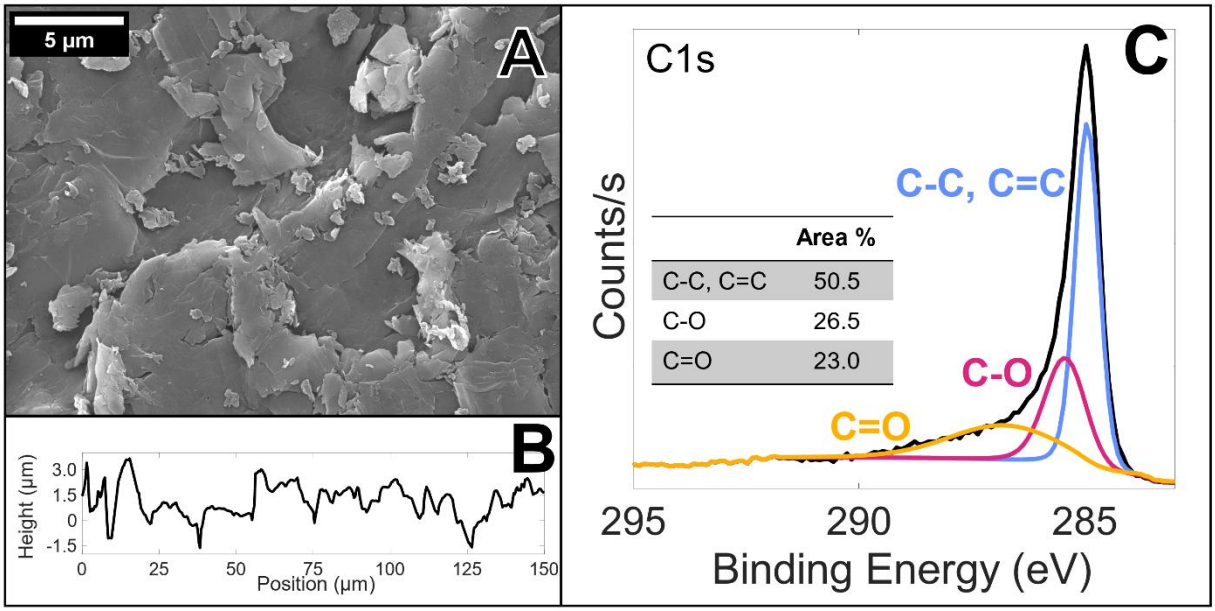

Figure 1. **(A)** Scanning electron micrograph at 5,000x magnification of bare TPE surface at 10.0 kV accelerating voltage. **(B)** Representative roughness profile of the TPE surface, R_{RMS} = 0.776 µm and R_A = 0.575 µm. **(C)** XPS high resolution C1s spectrum of TPE surface.

The equation (**Equation 1**) describing the value of the peak current for a monoelectronic reversible redox couple was used to determine the electroactive surface area using the peak current as a function of scan rate in cyclic voltammetry, where i_p is the peak current (A), F is

Faraday's constant ($C \cdot mol^{-1}$), R is the ideal gas constant ($J \cdot mol^{-1} \cdot K^{-1}$), T is temperature (K), A is the electrode electroactive area (cm^2), D is the diffusion coefficient ($cm \cdot s^{-1}$), C is the concentration (M), and v is the scan rate ($V \cdot s^{-1}$).[37]

$$i_p = 0.4463 \left(\frac{F^3}{RT}\right)^{\frac{1}{2}} A D^{\frac{1}{2}} C v^{\frac{1}{2}} \qquad \textbf{(Equation 1)}$$

Ferri/ferrocyanide ($Fe(CN)_6^{3-/4-}$) and ferrocenedimethanol ($Fc(MeOH)_2$) were used as complementary redox probes; $Fe(CN)_6^{3-/4-}$ being an inner-sphere electron transfer probe and $Fc(MeOH)_2$ an outer-sphere electron transfer probe, giving information on both electrode surface state and kinetic of electron transfer.[38] Cyclic voltammograms and the resulting peak current versus the square root of the scan rate plots are shown in **Figure S3**. The diffusion coefficients for $Fe(CN)_6^{3-/4-}$ in 0.1 M KCl were calculated using Equation 1 and the peak currents from cyclic voltammetry at 1 mV/s and assuming the area to be equivalent to the geometric area (0.0707 cm^2). The values are in agreement with literature at $D_O = 5.66 \times 10^{-6}$ $cm^2 \cdot s^{-1}$ and $D_R = 6.89 \times 10^{-6}$ $cm^2 \cdot s^{-1}$ by running cyclic voltammetry at 5 mV/s.[39] Temperature was assumed to be 298 K to calculate the electroactive area of the working electrode as 0.0957 cm^2 for the oxidized species. The reduced species electroactive area was in agreement at 0.0846 cm^2. This is over 130% of the geometric area for the oxidized species, which is sensible given the rough surface observed in **Figure 1**. The electroactive area determined using the oxidized and reduced $Fc(MeOH)_2$ was 0.0776cm^2 (oxidized species) and 0.0685cm^2 (reduced species), which is roughly 110% of the geometric area for the oxidized species. These values were again calculated using the assumption of 298 K and diffusion constants of $D_R = 6.06 \times 10^{-6}$ $cm^2 \cdot s^{-1}$ and $D_o = 7.00 \times 10^{-6}$ $cm^2 \cdot s^{-1}$ calculated in the same manner as for $Fe(CN)_6^{3-/4-}$ in agreement with previous work.[40] Due to the surface sensitive nature of $Fe(CN)_6^{3-/4-}$, it was expected for the geometric area in $Fe(CN)_6^{3-/4-}$ to

be lower than that of $Fc(MeOH)_2$.[41] It is hypothesized that the difference in electroactive area between the two probes is the result of random variation in surface area of the TPEs.

After establishing the baselines for TPE behavior and surface characteristics, TPE surface functionalization was carried out by electroreduction of aryl diazonium salt produced in situ by reacting 4-(trimethylsilyl)ethynylaniline with sodium nitrite, forming a protected alkyl monolayer.[15, 26] Representative cyclic voltammograms (**Figure S5**) demonstrate that the grafting reaction proceeded comparably to previous reports.[16, 17, 28] The resulting surface shows a clear silicon signal compared to a bare electrode (**Figure 2**) confirming, in conjunction with electrochemical data, a TMS-protected 4-ethynylbenzene monolayer on the surface. The C1s high resolution XPS spectrum also shows a broadening of the C1s peak including a contribution from C-Si and C-N bonding at 284.9 eV and 285.19 eV respectively, with atomic compositions calculated as follows: C-Si: 10.2%, C-C, C=C: 15.0%, C-N: 20.5%, C-O: 7.9% and C=O: 46.4%. The increase in C=O relative atomic percent is probably due to the aqueous treatment of the electrode surface during electrochemical grafting. The C-N contribution has already been observed during aryl diazonium grafting and is attributed to the reaction of the diazonium cation with surface groups of the carbon electrode or grafting of azophenyl groups, formed from the one-electron reduction of the diazo functional group, directly at the electrode surface.[42-44]

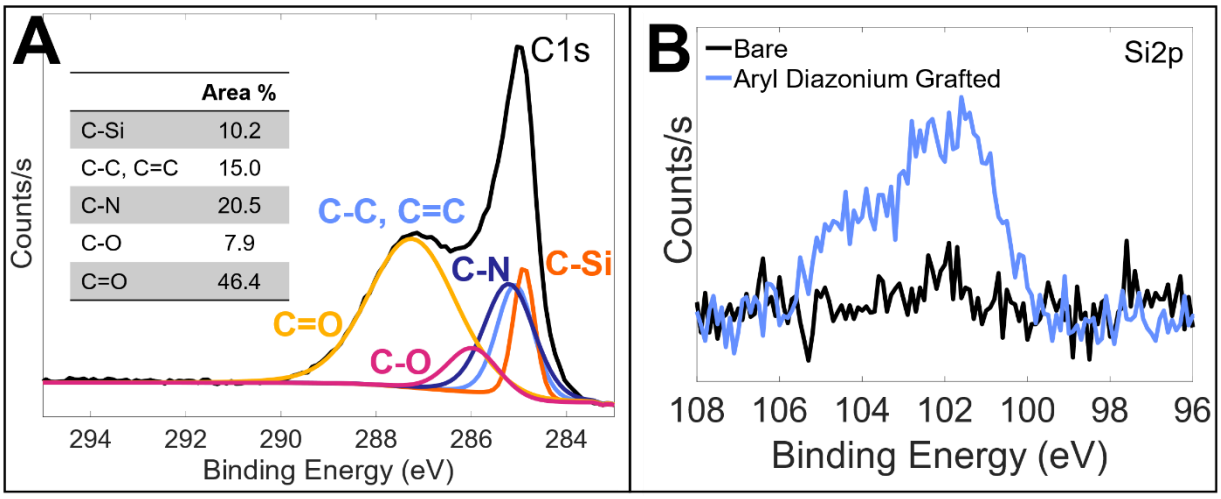

Figure 2. (A) C1s and **(B)** Si2p high resolution XPS spectra of functionalized TPE with 4-(trimethylsilyl)ethynylbenzene monolayer.

The diazonium salt solution concentration was varied from 0 mM to 10 mM (**Figure S6**) and the resulting electrochemical behavior of the functionalized TPE was evaluated via cyclic voltammetry in solution containing $Fc(MeOH)_2$ or $Fe(CN)_6^{3-/4-}$ redox probes. **Figure 3** shows the representative CVs for $Fc(MeOH)_2$ and $Fe(CN)_6^{3-/4-}$ redox probes. The CVs obtained in $Fe(CN)_6^{3-/4-}$ confirm a complete coverage of the TPE surface, with no pinholes or defects, for aryl diazonium concentration as low as 0.5 mM, while in $Fc(MeOH)_2$ no significant change can be observed. This is indicative of a very thin layer deposition as observed previously.[15] At 0.05 mM (**Figure S6**), there is a significant increase in reduction/oxidation of $Fe(CN)_6^{3-/4-}$ indicating a disperse monolayer. The well-structured monolayer is a benefit of completing the aryl diazonium grafting to functionalize the electrode surface prior to further functionalization. In an alternative situation, where a diazonium functionalized biotin compound is directly electrografted, there runs the probability that a disordered multilayer will form.[15] The 0.5 mM 4-(trimethylsilyl)ethynylbenzene diazonium solution was used for the remainder of the work,

reducing reagent cost (compared to 10 mM), but maintaining a consistent and complete functionalization of the surface.

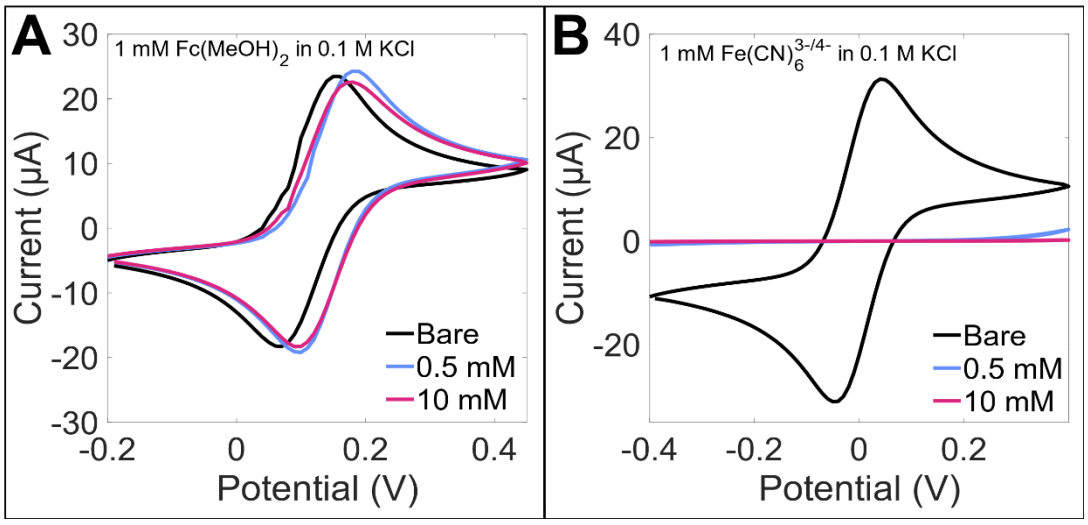

Figure 3. Representative cyclic voltammograms (**A)** 1 mM $Fc(MeOH)_2$ in 0.1 M KCl or (**B)** 1 mM $Fe(CN)_6^{3-/4-}$ in 0.1 M KCl on modified electrodes with 0.5 or 10 mM of diazonium salt solution grafted to the surface via electroreduction. Potential are given versus carbon pseudo reference.

From the voltammograms of $Fc(MeOH)_2$ (**Figure S7A and C**) we could derive an apparent electroactive area of the electrode before and after modification. The oxidized species electroactive area is 0.0708 cm^2 which is an 9% decrease from the bare surface area, which effectively does not impact the proportion of electroactive area percentage of the geometric area. The reduced species electroactive area is 0.0751 cm^2 which is an increase of approximately 10% from the bare surface and also not an appreciable change from the percent of the geometric area. The results indicate that the electrode modifications do not significantly impede the rate of electron transfer with ferrocene dimethanol, which is beneficial when considering biosensing applications.

Removing the TMS protecting group is the next phase and is critical for freeing the ethynyl group for click chemistry. While using TBAF in tetrahydrofuran has been shown to be highly successful, TPEs are not compatible with organic solvents.[16] Thus sodium hydroxide was used to remove the protecting group.[45] Deprotection conditions were optimized (**Figure S8**) and sonicating the electrodes in 1M NaOH for 20 min is effective in the removal of the TMS protection group. Cyclic voltammograms in **Figure 4** show that some $Fe(CN)_6^{3-/4-}$ signal is recovered after deprotection, while $Fc(MeOH)_2$ signal is largely unaffected. The signal suppression of $Fe(CN)_6^{3-/4-}$ despite deprotection is expected due to the small protecting group lending to a dense packing of the monolayer.[46]

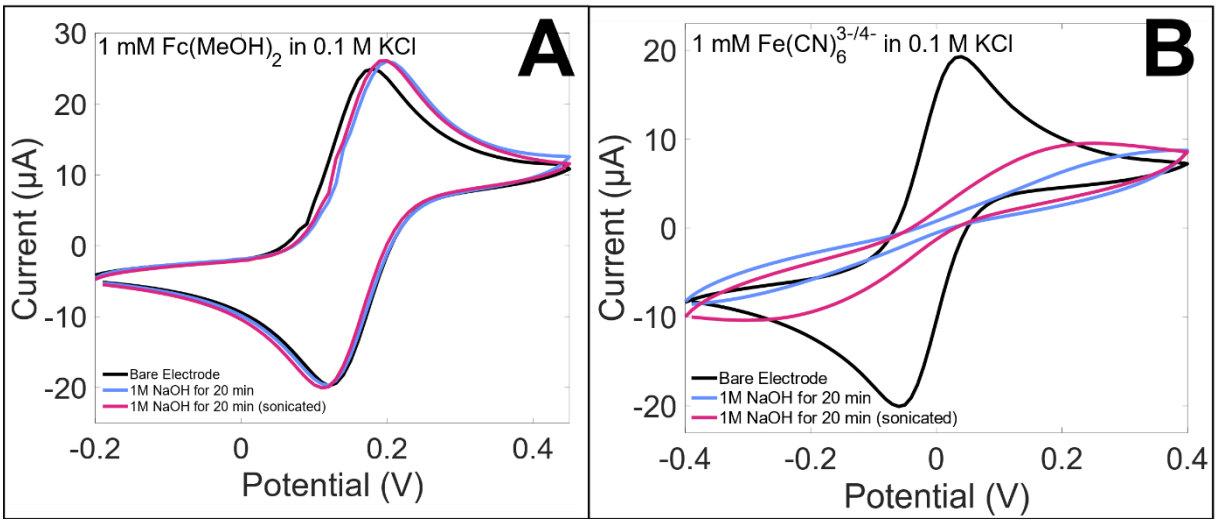

Figure 4. Representative cyclic voltammograms in (**A**) 1 mM $Fc(MeOH)_2$ in 0.1 M KCl or (**B**) 1 mM $Fe(CN)_6^{3-/4-}$ in 0.1 M KCl of bare (black curves) and functionalized TPEs deprotected using 1M NaOH solution for 20 min with (magenta curves) and without sonication (blue curves).

Upon freeing the alkyne moiety for the click chemistry reaction, a short diazido-PEG linker (N_3-PEG3-N_3) was introduced by click chemistry reaction, followed by the addition of ferrocenyl moieties through a second click chemistry reaction, resulting in a surface bound redox probe. The successful bonding of ferrocenyl moieties is observed both by electrochemical means

(**Figure 5A**) and by the appearance of a new signal at 709.5 eV in the XPS survey spectrum attributed to Fe2p (**Figure 5B**). From the area under the oxidation peak, the surface concentration of immobilized ferrocene (Γ_{Fc}) was determined.[47] At a scan rate of 10 mV·s^{-1}, the Γ_{Fc} was determined to be (1.0 ± 0.2) × 10^{-10} mol·cm^{-2}. This value is comparable to those reported for a similar approach on glassy carbon and pyrolytic graphite edge electrodes, (3.3 ± 0.9) × 10^{-10} and (14.3 ± 1.0) × 10^{-10} mol·cm^{-2} respectively.[47] This value is especially reasonable when considering the possible impact of the diazido-PEG linker used to immobilize the ferrocenyl moieties.

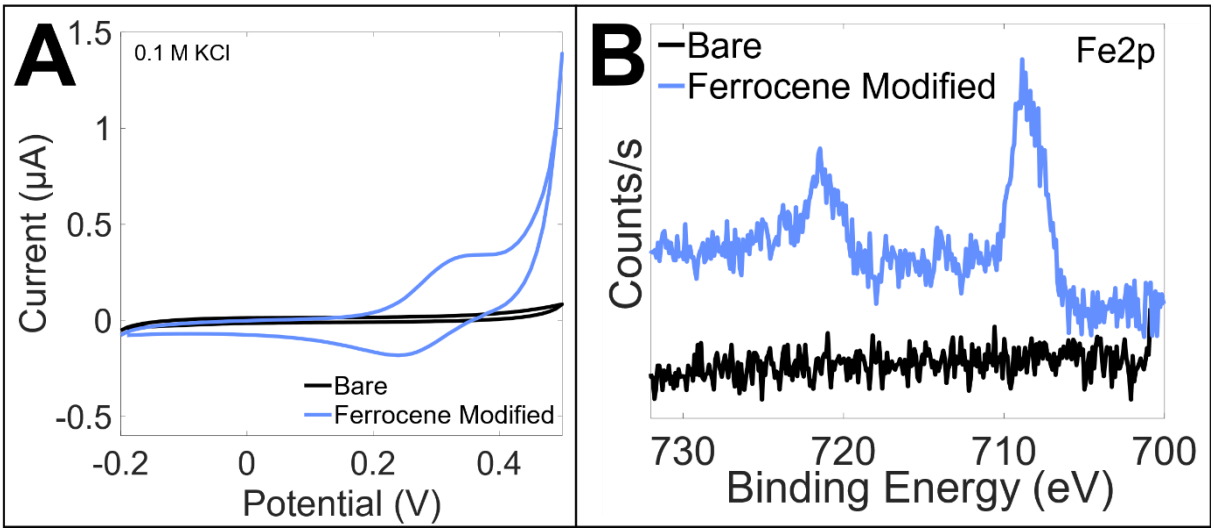

Figure 5. (**A**) Representative cyclic voltammograms of bare (black curve) and ferrocenyl functionalized (blue curve) TPE by click chemistry. Potential are given versus carbon pseudo-reference and scan rate = 10 mV·s^{-1}. (**B**) Fe2p high resolution XPS spectra of bare (black curve) and ferrocenyl functionalized (blue curve) TPE by click chemistry.

Upon demonstrating the success of clicking ferrocene to the surface, N_3-PEG3-biotin was clicked to the electrode surface, following diazonium electrografting. Representative CVs following the stepwise TPE modification (**Figure S9**) show the decrease in electron transfer at

the surface with $Fe(CN)_6^{3-/4-}$. The first step is from bare electrode to grafted and the near total suppression of electron transfer is seen. After deprotection, the signal is recovered and the subsequent step to click N_3-PEG3-biotin to the surface causes the signal to decrease as expected. To evaluate the quantity of biotin that was clicked onto the surface, the apparent electroactive area was determined considering the oxidation of $Fc(MeOH)_2$ at different scan rates (**Figure S10**) with **Eq 1** once again. In this estimation, we consider that the surface covered by PEG3-biotin is blocking for the oxidation of $Fc(MeOH)_2$. The oxidized species electroactive area was 0.0529 cm^2 which is a 27% decrease from that of the grafted electrode and 32% decrease from the bare electrode, thus the binding of the N_3-PEG3-biotin does not significantly impede electron transfer when using $Fc(MeOH)_2$.

Ultimately, the use of TPEs as an immunosensor requires the immobilization of a biorecognition element, such as an antibody to the surface. The confirmed presence of biotin clicked to the surface gave a point for streptavidin conjugation. Preliminary tests with cyclic voltammetry (**Figure S9**) showed the suppression of oxidation and reduction of $Fe(CN)_6^{3-/4-}$ as expected. It is seen that the signal on a streptavidin modified electrode is significantly lower than the negative control (N_3-PEG3-biotin modified electrode incubated in PBS only). Surprisingly, when streptavidinated-IgG antibody was bound to the biotin clicked surface, the resulting voltammogram shows higher signal than any of the modification steps. This behavior was further investigated by electrochemical impedance spectroscopy (EIS) (**Figure 6**). As expected, the data mirrors the CV results. The charge transfer resistance, R_{ct}, was calculated by the equivalent circuit shown in **Figure 6B** which is based on modified electrode equivalent circuits for electrodes with surface modification.[48-51] The R_{ct} values represented by the bar chart in **Figure 6B** correspond to R3 in the equivalent circuit and the average percent error of the fit was less

than 5% across all conditions (SI Table 1). The R_{ct} increases upon the addition of streptavidin compared to the control of phosphate buffered saline (PBS) yet decreases substantially when streptavidinated antibody is bound instead. Streptavidin is roughly 5 nm in diameter and is expected to pack much more tightly than the streptavidin-antibody complex in which the antibody portion alone is upwards of 14 nm at the longest side.[52, 53] Further, it is hypothesized that the streptavidin-antibody conjugate disrupts the PEG3-biotin monolayer on the surface creating gaps for the redox probe, $Fe(CN)_6^{3-/4-}$, to perform electron transfer more effectively at the electrode surface.

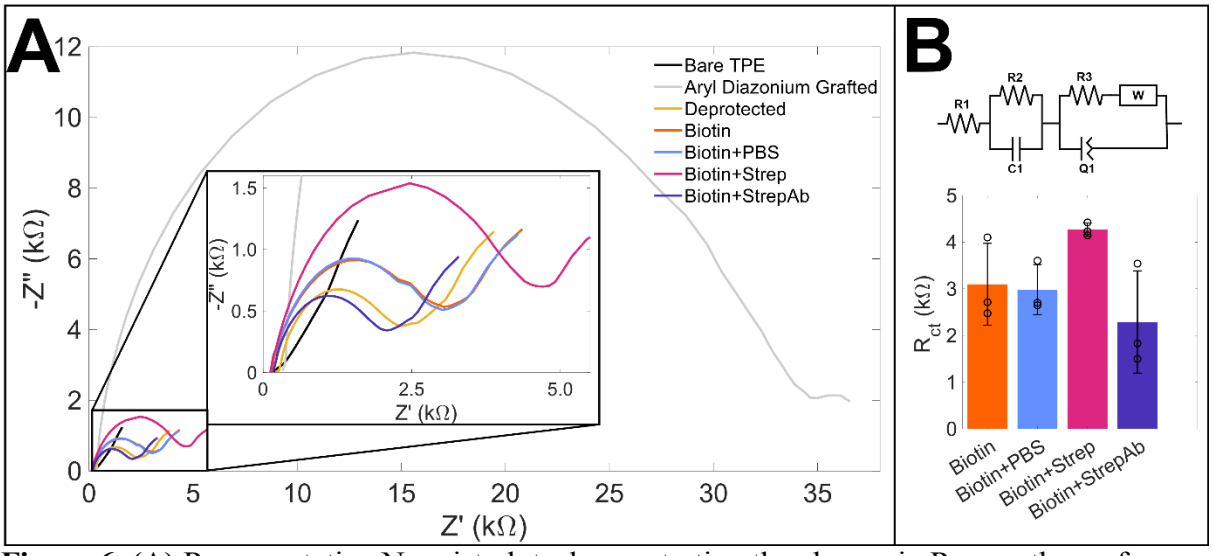

Figure 6. (A) Representative Nyquist plots demonstrating the change in R_{ct} as a the surface groups change. **(B)** EIS equivalent circuit and resulting calculated R_{ct} values (n=3) where the error bars represent standard deviation.

Further support that demonstrates the successful conjugation of streptavidin to the surface was achieved via scanning electrochemical microscopy (SECM) using $Fe(CN)_6^{4-}$ as the redox probe (**Figure 7**). On the bare electrode, approach curves show positive feedback (**Figure 7A**) indicating electron transfer between the TPE surface and $Fe(CN)_6^{4-}$ in solution. The increase in

current is relatively small, likely due to the rugosity of the surface impeding the approach of the SECM tip. A 200 μm square map of the bare electrode surface shows areas of higher and lower activity due to the surface roughness, but the whole surface demonstrates positive feedback indicating that there are no insulating zones on the bare TPE surface. After modifying the TPE with N_3-PEG3-biotin, negative feedback is observed across the whole surface shown in **Figure 7B**, corresponding with full coverage of the electrode preventing electron transfer. Approach curves for both the bare and N_3-PEG3-biotin modified electrodes are consistent within groups regardless of the approach location. Streptavidin was bound to the N_3-PEG3-biotin modified surface and the resulting surface is shown to be highly heterogenous with some areas giving positive feedback and some giving negative (**Figure 7C**). However, when streptavidin-antibody is immobilized onto the TPE instead, the surface regains positive feedback across the surface. The culmination of the data further supports the hypothesis that binding the relatively large streptavidin-antibody complex creates disruptions in the modification layers to facilitate the electron transfer at the TPE surface. **Scheme 2** illustrates the hypothesis on a molecular level where the bulkier streptavidin-antibody structure may cause greater gaps in the surface modifications allowing more $Fe(CN)_6^{3-/4-}$ to interact with the surface.

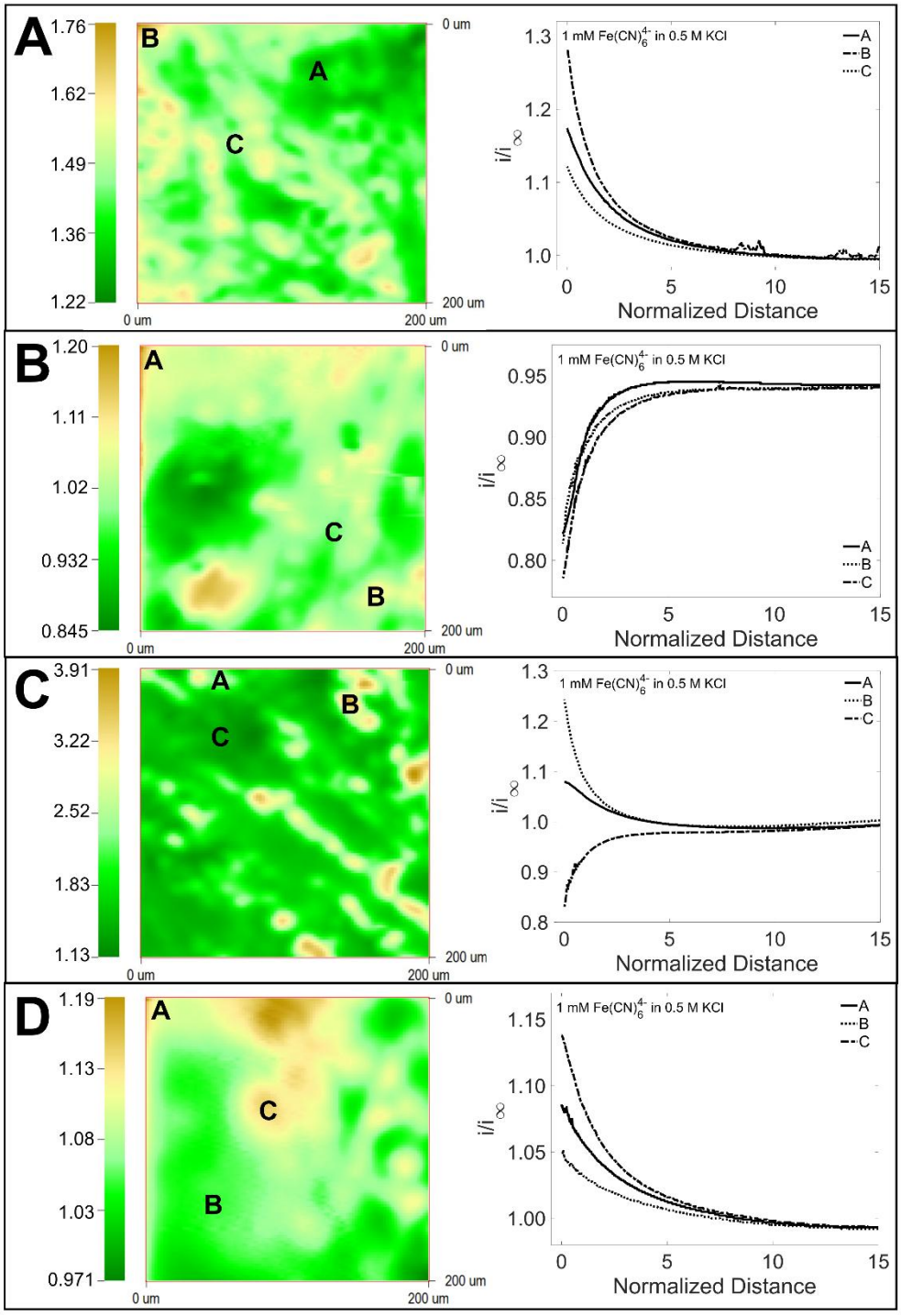

Figure 7. SECM maps and representative (n=3) probe approach curves taken in 1 mM ferrocyanide in 0.5 M KCl of 200 μm square sections of **(A)** bare electrodes, **(B)** N_3-PEG3-biotin modified electrodes, **(C)** streptavidin immobilized on electrodes, and **(D)** streptavidinated

antibody immobilized on electrodes. Average currents for the maps are 1.18 ± 0.08 µA, 1.20 ± 0.05 µA, 1.46 ± 0.23 µA, and 1.21 ± 0.05 µA respectively, with no statistical difference. All reported currents are normalized against the infinite current.

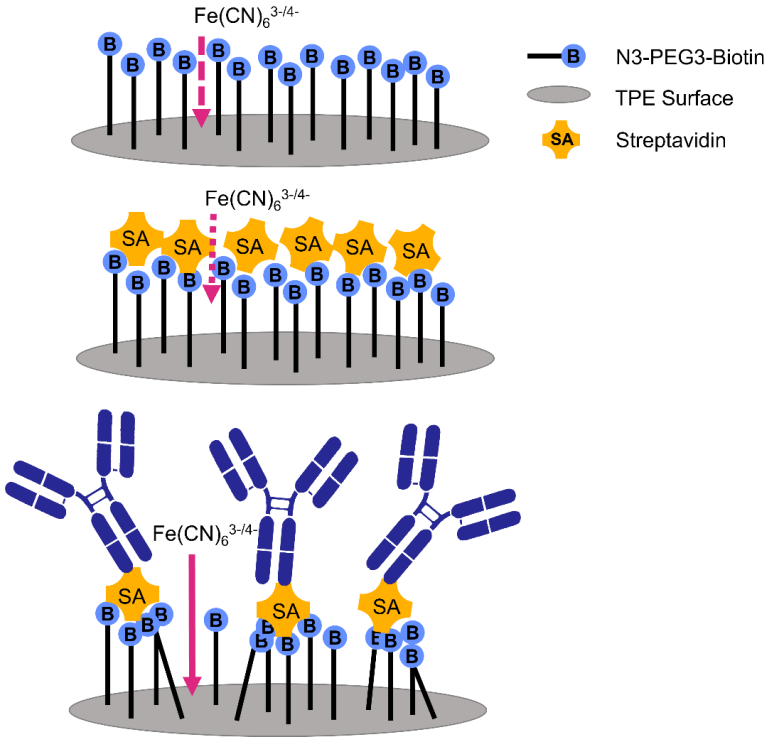

Scheme 2. Hypothesized molecular-level behavior of modified TPEs with the binding of streptavidin (SA) and streptavidin-antibody to N_3-PEG3-biotin modified TPEs.

Confirmation of streptavidin-antibody bound to the surface was made via XPS (**Figure 8**) where the C1s high resolution spectra demonstrate the changes in surface chemistry. Both biotin and streptavidin-antibody modified TPEs show the presence of increased nitrogen and sulfur over the bare electrode as expected due to the formation of the triazole linkage with N_3-PEG3-biotin and protein composition.[54-56] Most XPS analysis penetrates 5-10 nm into the sample surface; hence, the relative reduction in C-S and C-N bonding in the streptavidin-antibody decorated surface over the biotin clicked surface indicates the biotin structure being hidden by

the comparatively large protein layer.[56-58] The XPS data supports the electrochemical data demonstrating that streptavidin-antibody is successfully bound to TPEs modified with N_3-PEG3-biotin via click chemistry following diazonium electrografting for immunosensing applications.

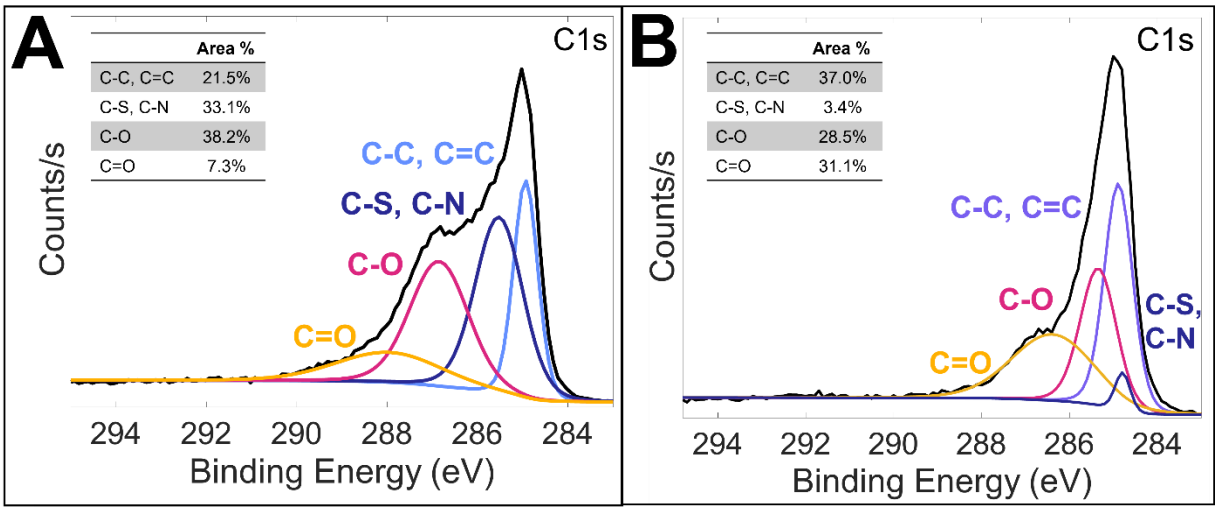

Figure 8. Deconvoluted XPS C1s high resolution spectra for **(A)** N_3-PEG3-biotin clicked and **(B)** streptavidin-antibody modified electrodes.

CONCLUSION

Here it has been shown that diazonium grafting followed by click chemistry is successful for adding biotin functionalization to TPEs, creating an easily customizable platform for biosensing. Electrochemical techniques and XPS were used to determine surface coverage of the diazonium monolayer, clicked N_3-PEG3-biotin, and to validate each step of the modification procedure. We demonstrated that the modification is successful and binding of large complexes, such as streptavidin-antibody conjugation, is believed to disrupt the modification layer, increasing the observed current in a surface sensitive redox probe. The multi-step approach used herein allows for a uniform monolayer to form in the aryl diazonium grafting step followed by highly customizable functionalization via click chemistry for a stable, biotinylated TPE. This work

provides an exciting basis for expanding the applicability of TPEs, which can be a better choice of electrode compared to expensive metal electrodes and more robust than SPCEs.

ASSOCIATED CONTENT

Supporting Information: The following are available free of charge: cyclic voltammograms for optimization steps not shown in main text, additional XPS spectra, and SECM maps with probe approach curves. (PDF)

AUTHOR INFORMATION

Corresponding Author

*Email: chuck.henry@colostate.edu

Author Contributions

B. M. collected and analyzed the data within this manuscript under the direct guidance from C. S. H. in collaboration with Y. L. and P. H. The manuscript was written by B. M. with edits and contributions from C. S. H., Y. L., and P. H.

Funding Sources

Funding for B. M. and C. S. H. was provided by the National Institutes of Health through EB031510. Y. L. and P. H. were supported was by the CNRS IEA-International Emerging Actions “TPE-ELEC”. The authors declare no competing financial interest.

ACKNOWLEDGEMENTS

The authors wish to thank the Analytical Resources Core (RRID: SCR_021758) at Colorado State University for instrument access, training, and assistance with sample analysis for SEM and XPS characterizations, particularly Dr. Rebecca Miller. The authors also wish to thank

Guilhem Pignol and Trung Nghia Nguyen Le for their assistance with SECM at the University of Rennes.

REFERENCES

1. Klunder, K. J.; Nilsson, Z.; Sambur, J. B.; Henry, C. S., Patternable Solvent-Processed Thermoplastic Graphite Electrodes. *Journal of the American Chemical Society* **2017,** *139* (36), 12623-12631.
2. Ozer, T.; Henry, C. S., All-solid-state potassium-selective sensor based on carbon black modified thermoplastic electrode. *Electrochimica Acta* **2022,** *404*, 139762.
3. Noviana, E.; Klunder, K. J.; Channon, R. B.; Henry, C. S., Thermoplastic Electrode Arrays in Electrochemical Paper-Based Analytical Devices. *Analytical Chemistry* **2019,** *91* (3), 2431-2438.
4. McCord, C. P.; Summers, B.; Henry, C. S., Simultaneous Analysis of Ascorbic Acid, Uric Acid, and Dopamine at Bare Polystyrene Thermoplastic Electrodes. *ChemElectroChem* **2022,** *9* (11), e202101600.
5. Ozer, T.; McCord, C.; Geiss, B. J.; Dandy, D.; Henry, C. S., Thermoplastic Electrodes for Detection of Escherichia coli. *Journal of The Electrochemical Society* **2021,** *168* (4), 047509.
6. Clark, K. M.; Henry, C. S., Thermoplastic Electrode (TPE)-based Enzymatic Glucose Sensor Using Polycaprolactone-graphite Composites. *Electroanalysis* **2021,** *n/a* (n/a).
7. Danczyk, R.; Krieder, B.; North, A.; Webster, T.; HogenEsch, H.; Rundell, A., Comparison of antibody functionality using different immobilization methods. *Biotechnology and Bioengineering* **2003,** *84* (2), 215-223.
8. Stanković, V.; Đurđić, S.; Ognjanović, M.; Antić, B.; Kalcher, K.; Mutić, J.; Stanković, D. M., Anti-human albumin monoclonal antibody immobilized on EDC-NHS functionalized carboxylic graphene/AuNPs composite as promising electrochemical HSA immunosensor. *Journal of Electroanalytical Chemistry* **2020,** *860*, 113928.
9. Sharafeldin, M.; McCaffrey, K.; Rusling, J. F., Influence of antibody immobilization strategy on carbon electrode immunoarrays. *Analyst* **2019,** *144* (17), 5108-5116.
10. Sehgal, D.; Vijay, I. K., A method for the high efficiency of water-soluble carbodiimide-mediated amidation. *Anal Biochem* **1994,** *218* (1), 87-91.
11. Nakajima, N.; Ikada, Y., Mechanism of Amide Formation by Carbodiimide for Bioconjugation in Aqueous Media. *Bioconjugate Chemistry* **1995,** *6* (1), 123-130.
12. Yáñez-Sedeño, P.; González-Cortés, A.; Campuzano, S.; Pingarrón, J. M., Copper(I)-Catalyzed Click Chemistry as a Tool for the Functionalization of Nanomaterials and the Preparation of Electrochemical (Bio)Sensors. *Sensors (Basel)* **2019,** *19* (10).
13. Guerrero, S.; Cadano, D.; Agüí, L.; Barderas, R.; Campuzano, S.; Yáñez-Sedeño, P.; Pingarrón, J. M., Click chemistry-assisted antibodies immobilization for immunosensing of CXCL7 chemokine in serum. *Journal of Electroanalytical Chemistry* **2019,** *837*, 246-253.
14. Cesbron, M.; Levillain, E.; Breton, T.; Gautier, C., Click Chemistry: A Versatile Method for Tuning the Composition of Mixed Organic Layers Obtained by Reduction of Diazonium Cations. *ACS Applied Materials & Interfaces* **2018,** *10* (44), 37779-37782.

15. Leroux, Y. R.; Fei, H.; Noël, J.-M.; Roux, C.; Hapiot, P., Efficient Covalent Modification of a Carbon Surface: Use of a Silyl Protecting Group To Form an Active Monolayer. *Journal of the American Chemical Society* **2010,** *132* (40), 14039-14041.
16. Leroux, Y. R.; Hui, F.; Noël, J.-M.; Roux, C.; Downard, A. J.; Hapiot, P., Design of Robust Binary Film onto Carbon Surface Using Diazonium Electrochemistry. *Langmuir* **2011,** *27* (17), 11222-11228.
17. Pinson, J.; Podvorica, F., Attachment of organic layers to conductive or semiconductive surfaces by reduction of diazonium salts. *Chemical Society Reviews* **2005,** *34* (5), 429-439.
18. Qi, H.; Li, M.; Zhang, R.; Dong, M.; Ling, C., Double electrochemical covalent coupling method based on click chemistry and diazonium chemistry for the fabrication of sensitive amperometric immunosensor. *Analytica Chimica Acta* **2013,** *792*, 28-34.
19. Guerrero, S.; Agüí, L.; Yáñez-Sedeño, P.; Pingarrón, J. M., Design of electrochemical immunosensors using electro-click chemistry. Application to the detection of IL-1β cytokine in saliva. *Bioelectrochemistry* **2020,** *133*, 107484.
20. An, Y.; Jin, T.; Zhu, Y.; Zhang, F.; He, P., An ultrasensitive electrochemical aptasensor for the determination of tumor exosomes based on click chemistry. *Biosensors and Bioelectronics* **2019,** *142*, 111503.
21. Xie, D.; Li, C.; Shangguan, L.; Qi, H.; Xue, D.; Gao, Q.; Zhang, C., Click chemistry-assisted self-assembly of DNA aptamer on gold nanoparticles-modified screen-printed carbon electrodes for label-free electrochemical aptasensor. *Sensors and Actuators B: Chemical* **2014,** *192*, 558-564.
22. Mishyn, V.; Rodrigues, T.; Leroux, Y. R.; Aspermair, P.; Happy, H.; Bintinger, J.; Kleber, C.; Boukherroub, R.; Knoll, W.; Szunerits, S., Controlled covalent functionalization of a graphene-channel of a field effect transistor as an ideal platform for (bio)sensing applications. *Nanoscale Horizons* **2021,** *6* (10), 819-829.
23. Rodrigues, T.; Mishyn, V.; Leroux, Y. R.; Butruille, L.; Woitrain, E.; Barras, A.; Aspermair, P.; Happy, H.; Kleber, C.; Boukherroub, R.; Montaigne, D.; Knoll, W.; Szunerits, S., Highly performing graphene-based field effect transistor for the differentiation between mild-moderate-severe myocardial injury. *Nano Today* **2022,** *43*, 101391.
24. Sánchez-Tirado, E.; González-Cortés, A.; Yáñez-Sedeño, P.; Pingarrón, J. M., Carbon nanotubes functionalized by click chemistry as scaffolds for the preparation of electrochemical immunosensors. Application to the determination of TGF-beta 1 cytokine. *Analyst* **2016,** *141* (20), 5730-5737.
25. Flavel, B. S.; Gross, A. J.; Garrett, D. J.; Nock, V.; Downard, A. J., A Simple Approach to Patterned Protein Immobilization on Silicon via Electrografting from Diazonium Salt Solutions. *ACS Applied Materials & Interfaces* **2010,** *2* (4), 1184-1190.
26. Hapiot, P.; Lagrost, C.; Leroux, Y. R., Molecular nano-structuration of carbon surfaces through reductive diazonium salts grafting. *Current Opinion in Electrochemistry* **2018,** *7*, 103-108.
27. Wu, T.; Fitchett, C. M.; Brooksby, P. A.; Downard, A. J., Building Tailored Interfaces through Covalent Coupling Reactions at Layers Grafted from Aryldiazonium Salts. *ACS Applied Materials & Interfaces* **2021,** *13* (10), 11545-11570.
28. Berg, K. E.; Leroux, Y. R.; Hapiot, P.; Henry, C. S., Increasing Applications of Graphite Thermoplastic Electrodes with Aryl Diazonium Grafting. *ChemElectroChem* **2019,** *6* (18), 4811-4816.

29. Hayat, A.; Sassolas, A.; Marty, J.-L.; Radi, A.-E., Highly sensitive ochratoxin A impedimetric aptasensor based on the immobilization of azido-aptamer onto electrografted binary film via click chemistry. *Talanta* **2013,** *103*, 14-19.
30. Hein, C. D.; Liu, X. M.; Wang, D., Click chemistry, a powerful tool for pharmaceutical sciences. *Pharm Res* **2008,** *25* (10), 2216-30.
31. Obaje, E. A.; Cummins, G.; Schulze, H.; Mahmood, S.; Desmulliez, M. P. Y.; Bachmann, T. T., Carbon screen-printed electrodes on ceramic substrates for label-free molecular detection of antibiotic resistance. *Journal of Interdisciplinary Nanomedicine* **2016,** *1* (3), 93-109.
32. Velický, M.; Toth, P. S.; Woods, C. R.; Novoselov, K. S.; Dryfe, R. A. W., Electrochemistry of the Basal Plane versus Edge Plane of Graphite Revisited. *The Journal of Physical Chemistry C* **2019,** *123* (18), 11677-11685.
33. Ba, O. M.; Marmey, P.; Anselme, K.; Duncan, A. C.; Ponche, A., Surface composition XPS analysis of a plasma treated polystyrene: Evolution over long storage periods. *Colloids and Surfaces B: Biointerfaces* **2016,** *145*, 1-7.
34. Hontoria-Lucas, C.; López-Peinado, A. J.; López-González, J. d. D.; Rojas-Cervantes, M. L.; Martín-Aranda, R. M., Study of oxygen-containing groups in a series of graphite oxides: Physical and chemical characterization. *Carbon* **1995,** *33* (11), 1585-1592.
35. Blyth, R. I. R.; Buqa, H.; Netzer, F. P.; Ramsey, M. G.; Besenhard, J. O.; Golob, P.; Winter, M., XPS studies of graphite electrode materials for lithium ion batteries. *Applied Surface Science* **2000,** *167* (1), 99-106.
36. Browne, M. M.; Lubarsky, G. V.; Davidson, M. R.; Bradley, R. H., Protein adsorption onto polystyrene surfaces studied by XPS and AFM. *Surface Science* **2004,** *553* (1), 155-167.
37. Hamann, C. H.; Hammett, A.; Vielstich, W., *Electrochemistry*. Second ed.; Wiley-VCH: 2007.
38. Chen, P.; McCreery, R. L., Control of Electron Transfer Kinetics at Glassy Carbon Electrodes by Specific Surface Modification. *Analytical Chemistry* **1996,** *68* (22), 3958-3965.
39. Moldenhauer, J.; Meier, M.; Paul, D. W., Rapid and Direct Determination of Diffusion Coefficients Using Microelectrode Arrays. *Journal of The Electrochemical Society* **2016,** *163* (8), H672-H678.
40. Mampallil, D.; Mathwig, K.; Kang, S.; Lemay, S. G., Redox Couples with Unequal Diffusion Coefficients: Effect on Redox Cycling. *Analytical Chemistry* **2013,** *85* (12), 6053-6058.
41. McCreery, R. L.; McDermott, M. T., Comment on Electrochemical Kinetics at Ordered Graphite Electrodes. *Analytical Chemistry* **2012,** *84* (5), 2602-2605.
42. Saby, C.; Ortiz, B.; Champagne, G. Y.; Bélanger, D., Electrochemical Modification of Glassy Carbon Electrode Using Aromatic Diazonium Salts. 1. Blocking Effect of 4-Nitrophenyl and 4-Carboxyphenyl Groups. *Langmuir* **1997,** *13* (25), 6805-6813.
43. Combellas, C.; Kanoufi, F.; Pinson, J.; Podvorica, F. I., Time-of-Flight Secondary Ion Mass Spectroscopy Characterization of the Covalent Bonding between a Carbon Surface and Aryl Groups. *Langmuir* **2005,** *21* (1), 280-286.
44. Laforgue, A.; Addou, T.; Bélanger, D., Characterization of the Deposition of Organic Molecules at the Surface of Gold by the Electrochemical Reduction of Aryldiazonium Cations. *Langmuir* **2005,** *21* (15), 6855-6865.
45. Wuts, P. G. M., Protection for the Alkyne-CH. In *Greene's Protective Groups in Organic Synthesis*, 5th ed.; John Wiley & Sons Inc.: Hoboken, New Jersey, 2014.

46. Leroux, Y. R.; Hapiot, P., Nanostructured Monolayers on Carbon Substrates Prepared by Electrografting of Protected Aryldiazonium Salts. *Chemistry of Materials* **2013,** *25* (3), 489-495.
47. Evrard, D.; Lambert, F.; Policar, C.; Balland, V.; Limoges, B., Electrochemical Functionalization of Carbon Surfaces by Aromatic Azide or Alkyne Molecules: A Versatile Platform for Click Chemistry. *Chemistry – A European Journal* **2008,** *14* (30), 9286-9291.
48. Magar, H. S.; Hassan, R. Y. A.; Mulchandani, A., Electrochemical Impedance Spectroscopy (EIS): Principles, Construction, and Biosensing Applications. *Sensors (Basel)* **2021,** *21* (19).
49. Najlaoui, D.; Echabaane, M.; Ben Khélifa, A.; Rouis, A.; Ben Ouada, H., Photoelectrochemical impedance spectroscopy sensor for cloxacillin based on tetrabutylammonium octamolybdate. *Journal of Solid State Electrochemistry* **2019,** *23* (12), 3329-3341.
50. Russell, C.; Ward, A. C.; Vezza, V.; Hoskisson, P.; Alcorn, D.; Steenson, D. P.; Corrigan, D. K., Development of a needle shaped microelectrode for electrochemical detection of the sepsis biomarker interleukin-6 (IL-6) in real time. *Biosensors and Bioelectronics* **2019,** *126*, 806-814.
51. Wang, B.; Jing, R.; Qi, H.; Gao, Q.; Zhang, C., Label-free electrochemical impedance peptide-based biosensor for the detection of cardiac troponin I incorporating gold nanoparticles modified carbon electrode. *Journal of Electroanalytical Chemistry* **2016,** *781*, 212-217.
52. Kuzuya, A.; Numajiri, K.; Kimura, M.; Komiyama, M., Single-molecule accommodation of streptavidin in nanometer-scale wells formed in DNA nanostructures. *Nucleic Acids Symp Ser (Oxf)* **2008,** (52), 681-2.
53. Tan, Y. H.; Liu, M.; Nolting, B.; Go, J. G.; Gervay-Hague, J.; Liu, G. Y., A nanoengineering approach for investigation and regulation of protein immobilization. *ACS Nano* **2008,** *2* (11), 2374-84.
54. Holzer, B.; Manoli, K.; Ditaranto, N.; Macchia, E.; Tiwari, A.; Di Franco, C.; Scamarcio, G.; Palazzo, G.; Torsi, L., Characterization of Covalently Bound Anti-Human Immunoglobulins on Self-Assembled Monolayer Modified Gold Electrodes. *Advanced Biosystems* **2017,** *1* (11), 1700055.
55. Mwanza, D.; Phal, S.; Nyokong, T.; Tesfalidet, S.; Mashazi, P., Electrografting of isophthalic acid monolayer and covalent attachment of antibody onto carbon surfaces: Construction of capacitive biosensor for methotrexate detection. *Electrochimica Acta* **2021,** *398*, 139360.
56. Nimni, M. E.; Han, B.; Cordoba, F., Are we getting enough sulfur in our diet? *Nutrition & Metabolism* **2007,** *4* (1), 24.
57. Gruian, C.; Vanea, E.; Simon, S.; Simon, V., FTIR and XPS studies of protein adsorption onto functionalized bioactive glass. *Biochimica et Biophysica Acta (BBA) - Proteins and Proteomics* **2012,** *1824* (7), 873-881.
58. Watts, J. F.; Wolstenholme, J., *An Introduction to Surface Analysis by XPS and AES*. Wiley: 2019.

Table Of Contents Graphic: